School of Mechanical Engineering

University of Tehran

Macro-Atomic Force Microscope

Summer Internship Report

Prof. Bahrami

Prof. Sadighi

Lab:

SEECS

Mahdis Rabbani

810697291

Summer 2021

Table of Content

Table of figures

Tables

Introduction

Gerd Binnig and Heinrich Rohrer invented the scanning tunneling microscope[1] in 1981, which was an analytical method for capturing surfaces in atomic scales and with high resolution. This invention brought up the invention of other scanning probe microscopes, which were based on scanning a sharp tip over a surface [1][2]. It works based on scanning a metal tip over the metallic surface of the sample and sensing the changes in the tunneling current or tunneling voltage, which is sensitive to the gap between the tip and the surface. The metal tip is fixed to a rectangular piezo drive. The control unit keeps the tunneling current constant by applying a voltage to the piezo in *z*-direction while the tip is scanning the surface in the *x*-*y* plate, which leads to the topography of the surface [3]. Although this approach results in perfect detection, its performance can be degraded if the tunneling surfaces are not clean [1].

Later on, Binnig came up with the idea of imaging the surfaces by the use of forces instead of the tunneling current. Binnig, Christoph Gerber of IBM, and Calvin Quate of Stanford calculated the stiffness of the equivalent spring between atoms and imaged atomic-scale topography by sensing angstrom-size displacements of a cantilever spring with weaker stiffness. This idea led to the invention of atomic force microscopy (AFM) [1]. In this method, the sample is laterally scanned by a microtip while the tip-sample interaction force or force derivative is measured simultaneously. This force is very sensitive to the gap between the tip and the sample and is measured by detecting the motion of a compliant object with a known force constant [4]. All AFMs have five essential components:

- A fine tip mounted on a flexible cantilever
- A way of measuring the deflection of the cantilever
- A feedback system
- A scanning system that moves the sample under the tip in a raster pattern
- A system for capturing the topography [1]

The cantilever is made of silicon, silicon oxide, or silicon nitride with a sharp tip. The deflection of the cantilever can be sensed by different methods, such as electron tunneling, optics, and capacitance [5]. Optical AFMs can be divided into two types. In the first type, the bending of the lever is measured by detecting the deflection of a light beam [1]. The optical system contains a light source and a photodetector. Images are captured by sensing the deflection of the lever or by using the deflection as feedback to keep the tip force constant and recording the tip movement. The sample is mounted on piezoelectric supports and the reflection of the beam is detected while there is a raster scan on the sample. Air turbulence leads to the lever deflection and makes noise which is avoided by the use of an enclosure [5][6]. In this type, the lever must be mirror-like.

The second type of optical detection is interferometry. In this type, the beam is focused on the back of the lever by a microscope objective, and its reflection is projected on a photodiode. There is also a reference beam, which is reflected from a flat (Figure 1). To adjust the phase of two reflection beams, the flat is connected to the microscope body via piezoelectric

[1] STM

tubes, as well. By the expansion of the two colinear, interfering beams a fringe pattern appears which is projected on the photodiode after some conditioning [4].

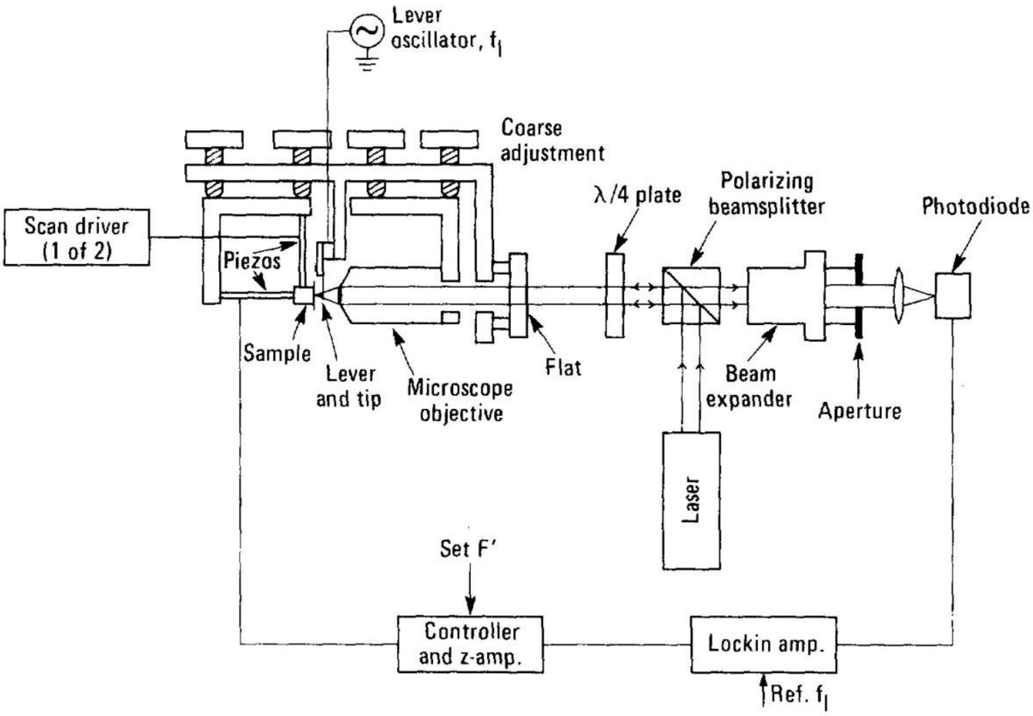

Figure 1: Scheme of an AFM with interferometry detection
(From R. Erlandsson, G. M. Mcclelland, C. M. Mate, and S. Chiang, reference 4)

The foremost advantage of this method is that the surface of the cantilever does not have to be mirror-like. Thus, it can be made of wire [1].

AFM modes

1. Contact Mode (Static Mode)

When the tip and sample are in continuous contact and have physical interaction while scanning, the AFM is in contact mode. This mode has two approaches: constant force and constant height. In the first approach, the deflection of the probe is maintained in a constant value and is used as a feedback parameter. This controls the intensity of the tip-sample interaction. This approach is used for imaging the surface [7]. The constant height approach uses the height of the cantilever concerning the sample as feedback.

2. Non-contact Mode

In this mode, there is no physical interaction between the sample surface and the tip. The cantilever is excited to oscillate near its resonance frequency and the tip is brought near the surface but there is no contact. The height of the sample is determined by the Van Der Waals forces in attractive and repulsive regimes.

3. Tapping Mode (Dynamic Mode or Intermittent Mode)

In this mode, the cantilever is excited by an external force and oscillates with a constant amplitude at a fixed frequency close to its resonance. The feedback can be based on the oscillation amplitude or frequency shift. As the tip approaches the surface, the physical contact between the tip and the sample changes the amplitude of the oscillation by causing a frequency shift. If the feedback is set to keep the amplitude constant, the AFM is in amplitude modulation (AM-AFM) which allows high resolutions [8][9]. On the other hand, in frequency modulation (FM-AFM), the output frequency of a constant amplitude oscillator changes by force gradient variations. The amplitude of the oscillating cantilever is maintained constant at a preset value with positive feedback. The change in frequency is detected by any analog FM demodulators [10][11].

Macro-AFM

The macro-scale atomic force microscopy (micro-AFM) is a variation of AFMs which operates in FM-AFM tapping mode. One significant difference in this variation is its electromagnetic self-sensing self-actuating probe. There is a scanning stage and a real-time controller to raster scan the sample. In the following sections, the hardware parts of the probe will be discussed [12].

Self-sensing Self-actuating Probe

A probe refers to a metallic cantilever, permanent magnet, and coil and is designed to track the sample surface in the *z*-direction. It is called self-sensing self-actuating since the mechanism for sensing the sample surface and the actuating mechanism are integrated i.e., despite regular scanning probes, the self-sensing probe does not need an optical beam to detect the cantilever bending. It determines the deflection of the cantilever by coil voltage signals. Moreover, the cantilever is excited with the Lorentz force between the magnet and the coil. Thus, no actuator is needed. The specifications of each component are mentioned below:

Table 1: Extract specifications of the parts in paper [12]

Cantilever:	Material:	Phosphorous bronze alloy 510
	Dimension:	38-mm long, 6.3-mm wide, and 0.2-mm thick (Water jet cutter)
Permanent magnet:	Grade:	Axially magnetized neodymium disc magnet N42
	Dimension:	5.1-mm diameter, 3.2-mm thickness (Epoxy bonded to the cantilever)
Coil (air-core):	Number of turns:	30 turns of 18-gauge magnet wire
Modal	First mode frequency	35.2 Hz

To rebuild the probe, firstly, the system including the lever and the magnet is designed in SOLIDWORKS. Pictures of these parts are shown in Figure 2. Since no magnet with desired dimensions exists in the market, the magnet is designed with a diameter of 5 mm and a height of 3 mm. In conclusion, the resonance frequency of the system no longer equals 35.2 Hz. Thus, modal analysis is carried out in ANSYS software (Figure 3) to identify the resonance frequency of the system.

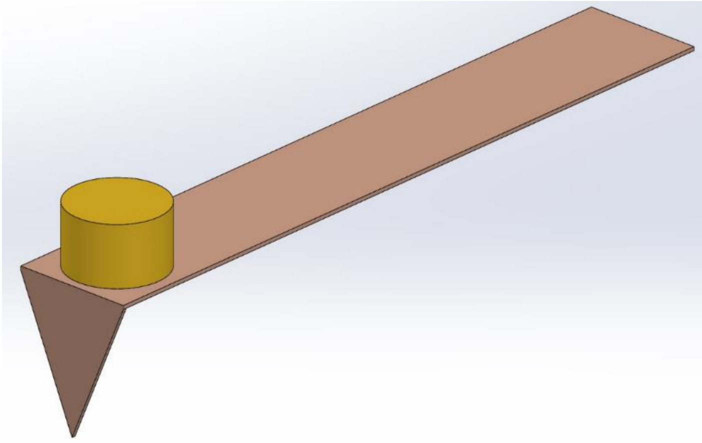

Figure 2: System of lever and magnet designed in SOLIDWORKS

The specification of the cantilever is given in Table 2. Note that we neglect the moment of inertia of the magnet in analytical calculations to avoid complexity.

Table 2: Lever specification

Length	38 mm
Width	6.3 mm
Thickness	0.2 mm
Moment of inertia	4.20×10^{-15} m^4
Module of elasticity	1.077×10^{11} Pa
Poisson's ratio	0.345
Density	8715 kg/m^3

The resonance frequency calculated in ANSYS is equal to 43.09 Hz which is 22% more than the desired amount. The reason may be the experimental errors or the slight differences in the amount of real and theoretical densities or stiffnesses.

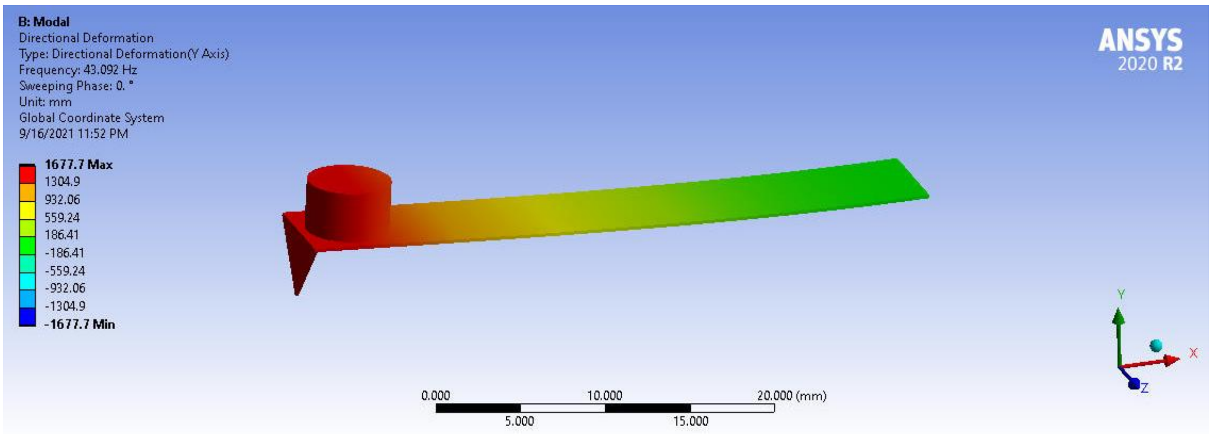

Figure 3: Calculating resonance frequency in ANSYS

To check the reliability of the results, the modal analysis is performed in COMSOL Multiphysics as well (Figure 4). The results of COMSOL closely resemble the results of

ANSYS. The resonance frequency in COMSOL equals 41.896 Hz. The error can be calculated as below:

$$err = \frac{43.09 - 41.896}{43.09} \times 100 = 2.77\%$$

This can collaborate the results are reliable. Therefore, we can assume the frequency of the oscillation of the cantilever is 42 Hz close to its resonance frequency.

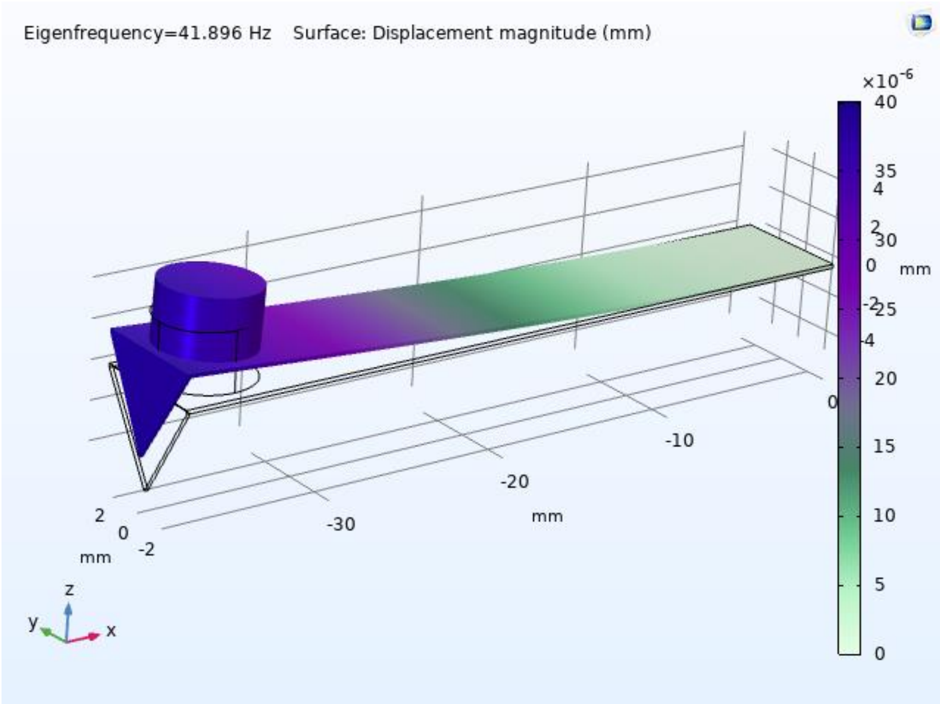

Figure 4: Calculating resonance frequency in COMSOL Multiphysics

As mentioned previously, the oscillation of the cantilever is created because of the harmonic magnetic force which the coil applies to the magnet. Thus, the current in the coil should be an alternating current[2]. The amplitude of the magnetic force is related to the amplitude of the current. So, if the force is specified, the current is determined as well. We assume the current is sinusoidal with a frequency of 42 Hz. In conclusion, the force and the displacement of the lever are sinusoidal with the same frequency (as desired). To clarify, consider a system, including the cantilever and the magnet, with the harmonic force as input and the displacement as output. The system is graphically illustrated in Figure 5.

$$F = \sin(\omega t) \longrightarrow \boxed{\text{system}} \longrightarrow d = \mathrm{M}\sin(\omega t + \varphi)$$

Figure 5: Scheme of the system

The parameters M and φ can be determined from the bode diagram of the system. The bode diagram can be plotted analytically or by simulation. In the analytical solution, we should

[2] AC

write the governing equations of the system and extract the transfer function for force input and displacement output. Equations are mentioned briefly mentioned below:

$$\frac{Z}{F_m} = \frac{1}{ms^2 + bs + (k + k_s)} \qquad [12]$$

$$Z_m = \frac{p^2 s}{ms^2 + bs + (k + k_s)} \qquad [12]$$

So:

$$Z = \frac{F_m Z_m}{p^2 s} \longrightarrow |Z| = \frac{|Z_m||F_m|}{p^2 \omega} \qquad (1)$$

Where F_m, Z_m, and Z represent the magnetic force, magnetically-induced impedance whose bode diagrams are given in [12], the displacement of the tip, and p equals 1.18×10^{-2} N/A. Equation 1 can be used later to validate the results.

In the second method, the bode diagram of the system is plotted in vibration simulator software such as ANSYS or COMSOL.

Frequency response of the cantilever

We have used ANSYS harmonic response study to plot the bode diagram. Firstly, the geometry of the system designed in SOLIDWORKS is imported to the ANSYS workbench. Then, the model is defined. In this study, we only need fixed support for the cantilever and a force at the end of the lever. This force represents the magnetic force applied to the magnet. To put it another way, we have separated the problem into two parts:

- The mechanical part:
  This part involves the oscillating cantilever and we want to find its bode diagram regardless of the source of the input force.

- The magnetic induction part:
  In the previous part, we have determined the required force for our desire displacement and in this part, we are trying to find the required alternating current which applies that required force to the magnet.

Since we are in the harmonic response study, we can specify the magnitude and phase of the force. The software simulates the model in a range of frequencies. We choose a magnitude and plot the frequency response of the displacement. Then, we can calculate the gain of the system by dividing the displacements by the force magnitude. We should notice that the force magnitude has an upper limit since the lever should remain in the elastic region. So, first of all, we carried out a static analysis to find the static force in which the displacement of the lever is 1 mm. The first approach is to use analytical formula as equation 2:

$$\delta = \frac{pl^3}{3EI} \qquad (2)$$

If we neglect the moment of inertia of the tip and magnet, the force required for 1-mm static deformation is equal to 0.0247 N. Thus, we can consider this force as the upper limit of the harmonic force magnitude. We can simulate the system in ANSYS as well. As the results shown in Figure 6, the maximum deformation is 0.971 mm, approximately 1 mm.

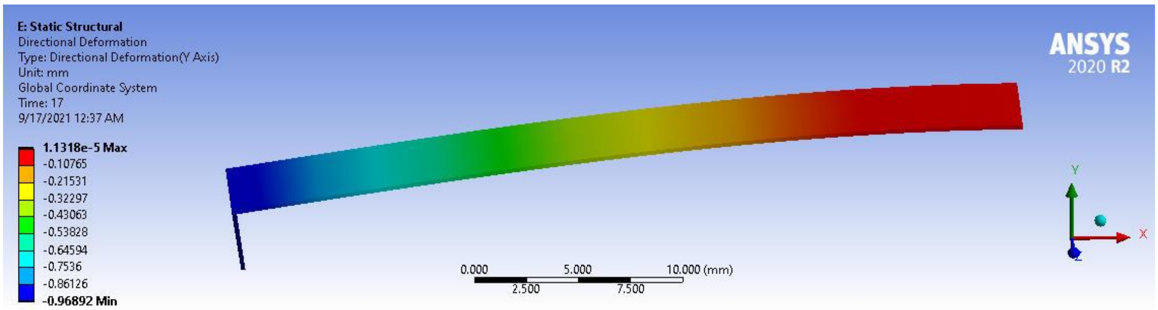

Figure 6: Static deformation of the cantilever

We assumed that the magnitude of the force is 0.005 N, which is way smaller than the upper bound and is reliable. Now, it is possible to simulate the harmonic response. The frequency response of the system is shown in Figure 7. As previously calculated, the first resonance mode occurs at about 43 Hz. We can calculate the gain of the system at 42 Hz. The gain plot is illustrated in Figure 8.

$$gain = \frac{d}{F} = \frac{3.5148}{0.005} = 702.96 \text{ mm/N}$$

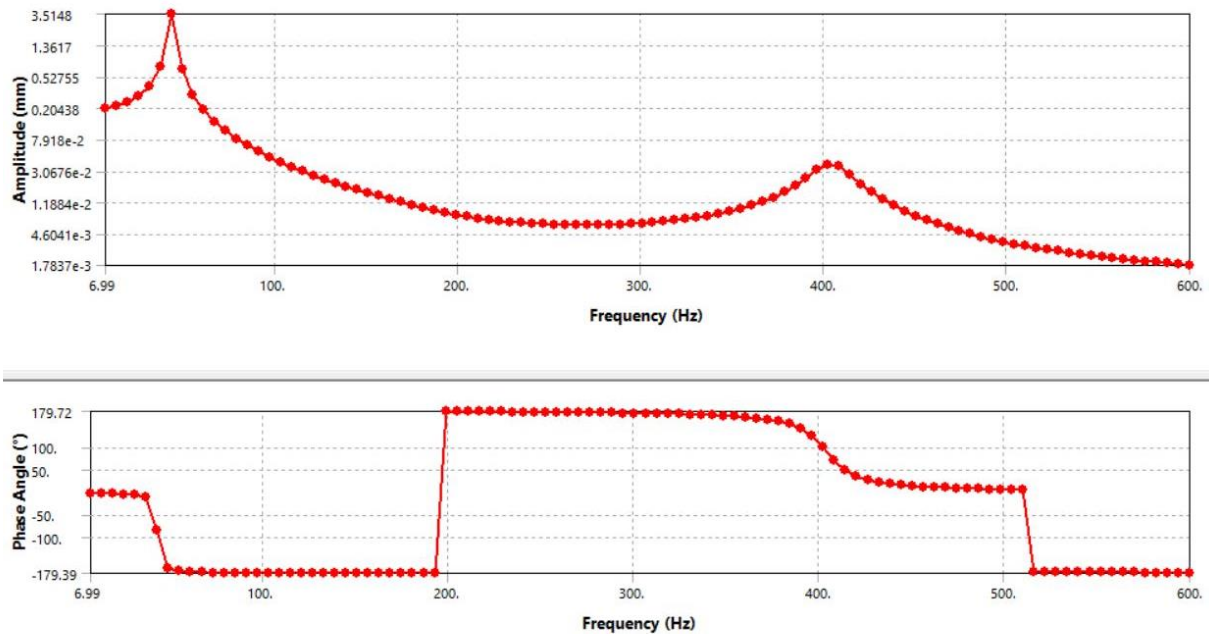

Figure 7: Frequency response of the system for the input force of 0.005 N

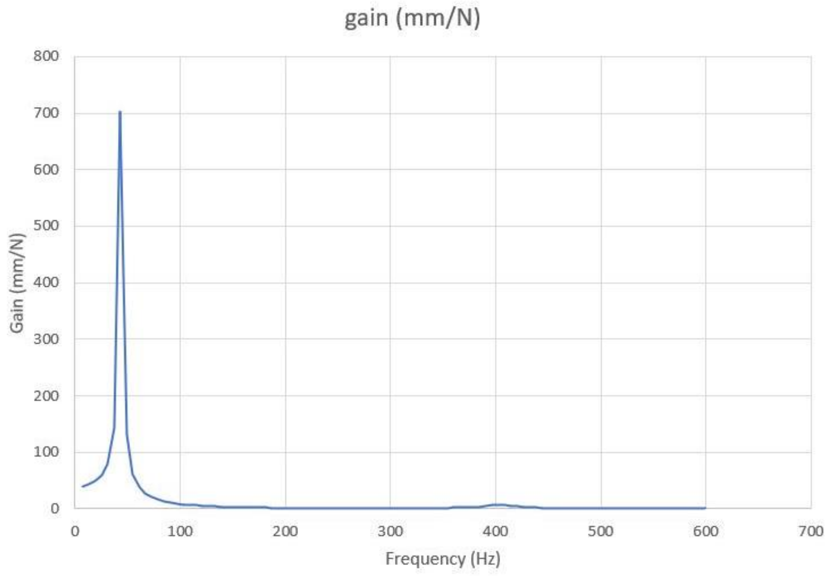

Figure 8: Gain of the mechanical part of the system

Now we can obtain that what force magnitude is required at 42 Hz to reach our desired displacement amplitude. The next step is to find the proper alternating current which can provide us with the desired force magnitude.

Frequency response of the coil

In this part, we are looking for the gain of the system, including coil and magnet, at 42 Hz. So, we can simulate the system in ANSYS Maxwell and find the force applied on the magnet (or the coil) which is the result of the change in the coil current. Since the magnetic force is closely related to the distance between the magnet and the coil, the kinematic of the magnet should be considered. If we neglect the effect of the cantilever on the magnet, which has damping and stiffness, the motion of the magnet will differ from its real motion. Thus, we should find the stiffness and damping of the cantilever. To find the stiffness we can use the governing equation and use Hooke's law:

$$\delta = \frac{Pl^3}{3EI} \longrightarrow P = \frac{3EI}{l^3}\delta$$

Hooke's law: $F = k\delta \longrightarrow k = \frac{3EI}{l^3}$

So, we can assume the stiffness is equal to 24.7 N/m. We assume the structural damping coefficient is 0.055 N. s/m as well. These values are being used in the Maxwell simulation as the mechanical transient conditions.

To carry out the simulation, first of all, the geometry of the system should be defined. Since both the coil and the magnet are cylindrical shapes, we can use the 2D axisymmetric option. This will speed up the simulation. The model designed in the software is shown in Figure 9. Note that two extra parts are needed for the simulation: the first one is a region in which the simulator has to solve the equation, and the second one is a band in which the magnet is allowed to move.

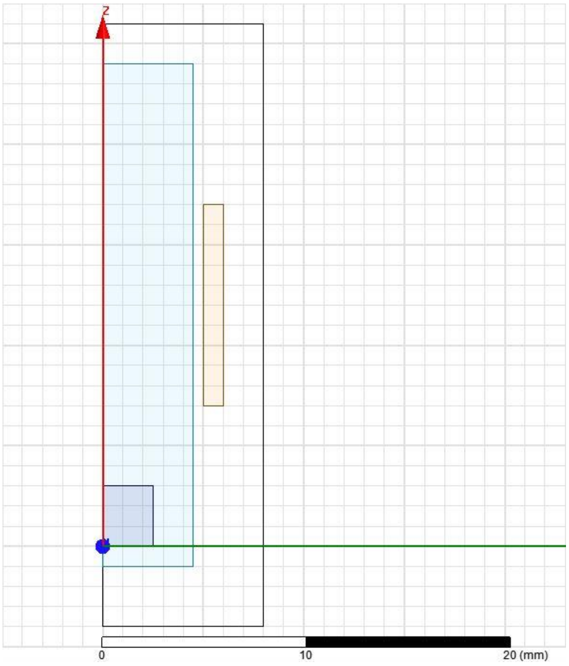

Figure 9: Geometry of the model designed in ANSYS Maxwell

After assigning desired materials to each part, we should define the coil. We define it as a one-conductor coil and then add it to a winding. We can define a parameter for frequency and define a parametric sweep to calculate the results for a range of frequencies and plot the frequency response as well. But, we just run the simulation for 42 Hz input current (Figure 10). Since the magnet should be able to move, we have to assign a band to the band part and specify the motion setup, which includes the time interval of the simulation. We must also assign a force from the parameter assignment part to the magnet so the simulator calculates the force applied to the magnet. We can specify the mesh setup at the end, but if we do not, the simulator, for one, will do that. When all parts are set, we can run the simulation.

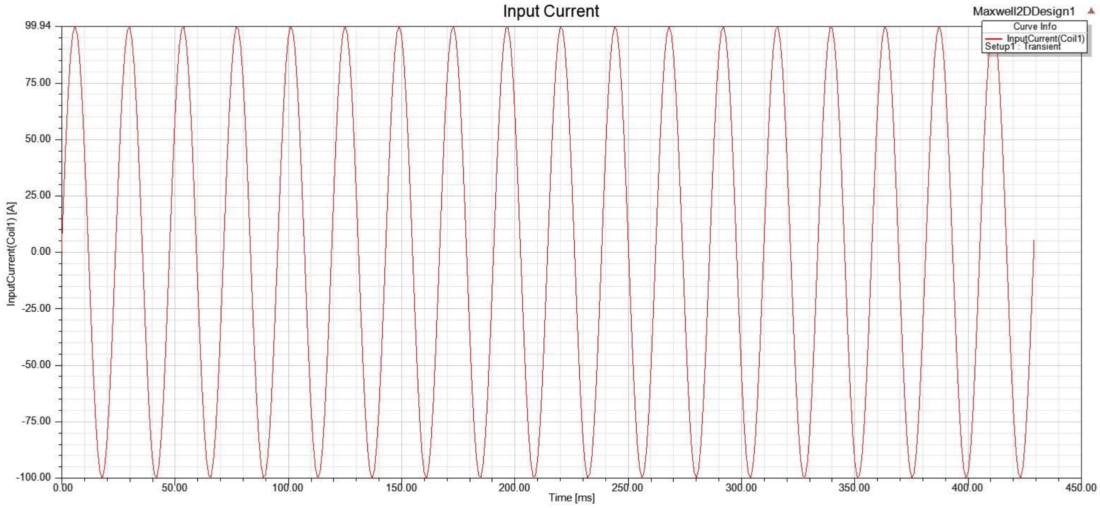

Figure 10: The input current of the coil

Note that in the analysis setup part of the software, we ought to define a range and a step time for saving the data points. In other words, the software has to sample the output data to draw the plots. Thus, due to the sampling theory [13], the step size should be smaller than one-half of the signal frequency which means that the sampling frequency should be at least twice the frequency of the signal. Here, the frequency of the current is 42 Hz. So, the step size should be less than 0.011 s. We defined a one-thousandth-second (0.001 s) step time in our simulation. The resultant force is illustrated in Figure 11.

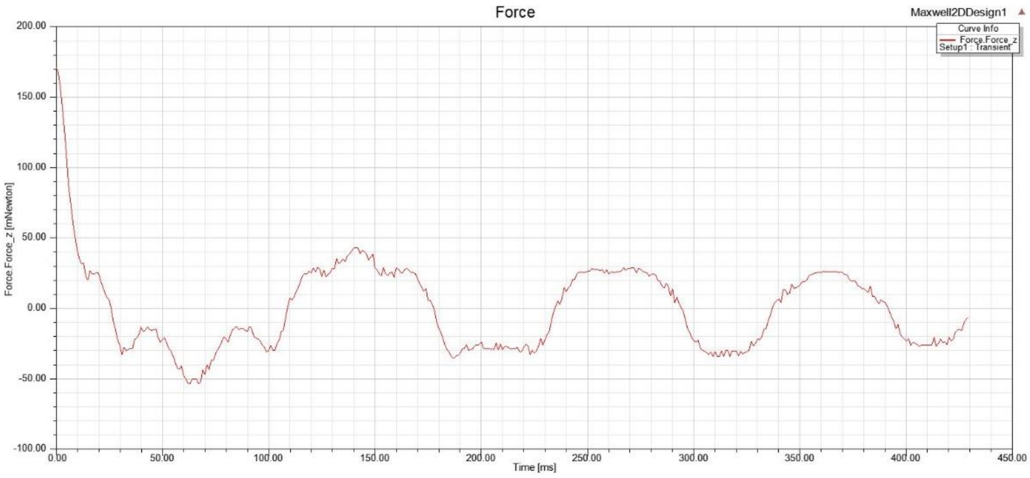

Figure 11: Force applied to the magnet at 42 Hz

Mechanical design

In this section, we designed a structure for assembling the probe on it. The structure is designed in SOLIDWORKS and is shown in Figure 12. As illustrated in the picture, the structure involves three parts:

1) The coil core:

   This part is a thin cylindrical shell on which the coil is mounted.

2) The coil holder:

   This is a standard unequal leg angle modified to locate the coil above the magnet. This part joins the rest of the microscope with an M5 hex bolt.

3) The base:

   This part is necessary to provide the lever with fixed support. The base is fastened to the coil holder with two socket screws and the lever is firmly clamped by a socket set screw.

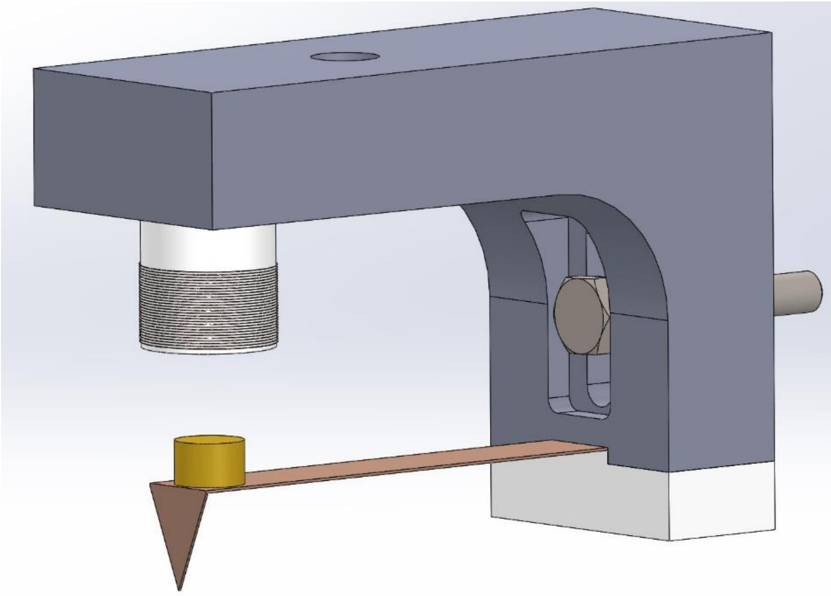

Figure 12: The probe and its holder designed in SOLIDWORKS

The exploded view of the entire system is given in Figure 13. Each part is introduced below:

1. Coil holder (unequal leg angle)
2. Coil core
3. Coil
4. Magnet
5. Cantilever
6. M5 Hex bolt
7. Base
8. M3 Socket screws
9. M3 Socket set screw

The technical drawings of the designed parts are available in Appendix *A*. Note that for the coil holder, we have found that the angle with a standard size of $100 \times 65 \times 10$ is appropriate [14].

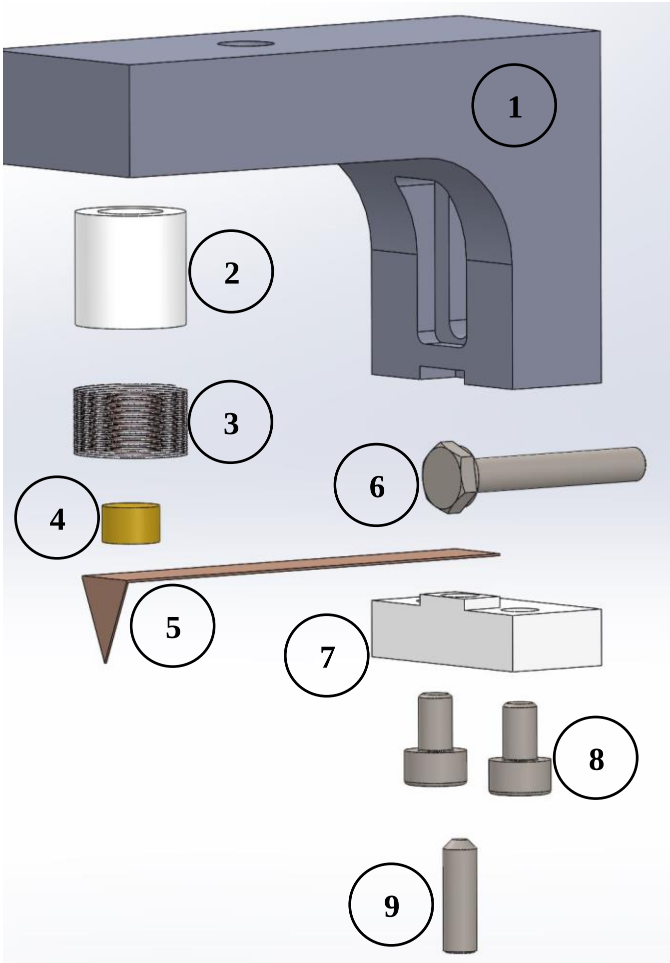

Figure 13: Exploded view of the system designed in SOLIDWORKS

References

[1] D. Rugar and P. Hansma, “Atomic Force Microscopy,” *Phys. Today*, vol. 43, no. 10, pp. 23–30, Oct. 1990, doi: 10.1063/1.881238.

[2] C. Gerber, G. Binnig, H. Fuchs, O. Marti, and H. Rohrer, “Scanning tunneling microscope combined with a scanning electron microscope,” *Rev. Sci. Instrum.*, vol. 57, no. 2, pp. 221–224, 1986, doi: 10.1063/1.1138973.

[3] G. Binnig and H. Rohrer, “Scanning Tunneling Microscopy,” *IBM J. Res. Dev.*, vol. 126, no. 1–3, pp. 236–244, 1983, doi: 10.1016/0039-6028(83)90716-1.

[4] R. Erlandsson, G. M. Mcclelland, C. M. Mate, and S. Chiang, “Atomic force microscopy using optical interferometry Atomic force microscopy using optical interferometry,” *J. Vac. Sci. Technol.*, vol. 266, no. 1988, pp. 0–5, 2014, doi: 10.1116/1.575440.

[5] S. Alexander *et al.*, “An atomic-resolution atomic-force microscope implemented using an optical lever,” *J. Appl. Phys.*, vol. 65, no. 1, pp. 164–167, 1989, doi: 10.1063/1.342563.

[6] N. A. Geisse, “AFM and combined optical techniques,” *Mater. Today*, vol. 12, no. 7–8, pp. 40–45, 2009, doi: 10.1016/S1369-7021(09)70201-9.

[7] G. J. Simpson, D. L. Sedin, and K. L. Rowlen, “Surface Roughness by Contact versus Tapping Mode Atomic Force Microscopy,” *Langmuir*, vol. 15, no. 4, pp. 1429–1434, 1999, doi: 10.1021/la981024a.

[8] R. Garcı, “Attractive and repulsive tip-sample interaction regimes in tapping-mode atomic force microscopy,” *Phys. Rev. B*, vol. 60, no. 7, pp. 4961–4967, 1999.

[9] M. Lee and W. Jhe, “General Theory of Amplitude-Modulation Atomic Force Microscopy,” vol. 036104, no. July, pp. 1–4, 2006, doi: 10.1103/PhysRevLett.97.036104.

[10] J. I. Kilpatrick *et al.*, “Frequency modulation atomic force microscopy in ambient environments utilizing robust feedback tuning,” *Rev. Sci. Instrum.*, vol. 80, no. 2, 2009, doi: 10.1063/1.3073964.

[11] T. R. Albrecht *et al.*, “Frequency modulation detection using highQ cantilevers for enhanced force microscope sensitivity,” *J. Appl. Phys.*, vol. 69, no. 2, 1991, doi: 10.1063/1.347347.

[12] D. Amin-Shahidi and D. Trumper, “Macro-scale atomic force microscope: An experimental platform for teaching precision mechatronics,” *Mechatronics*, vol. 31, pp. 234–242, 2015, doi: 10.1016/j.mechatronics.2015.08.007.

[13] R. S. Figliola and D. E. Beasley, “Theory and Design for Mechanical Measurements, Second Edition,” *Eur. J. Eng. Educ.*, vol. 20, no. 3, pp. 386–387, 1995, doi: 10.1080/03043799508928292.

[14] M. Korashy, S. Ibrahim, and M. Korashy, “Tables for Steel Constructions,” *Book*, vol. 1, p. 5, 2001.

Appendix A

Technical drawings of parts

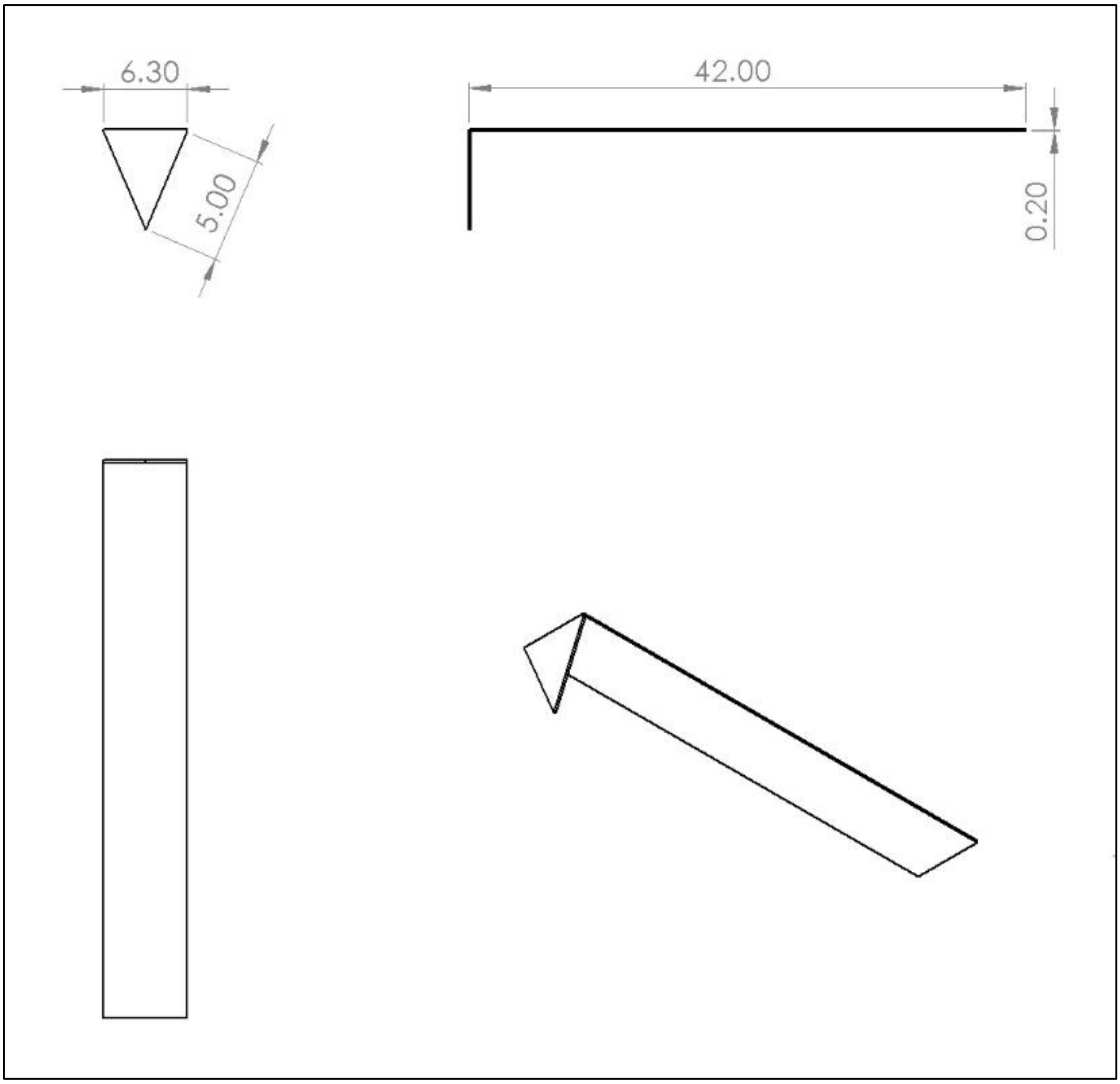

Figure 14: Drawing of the lever

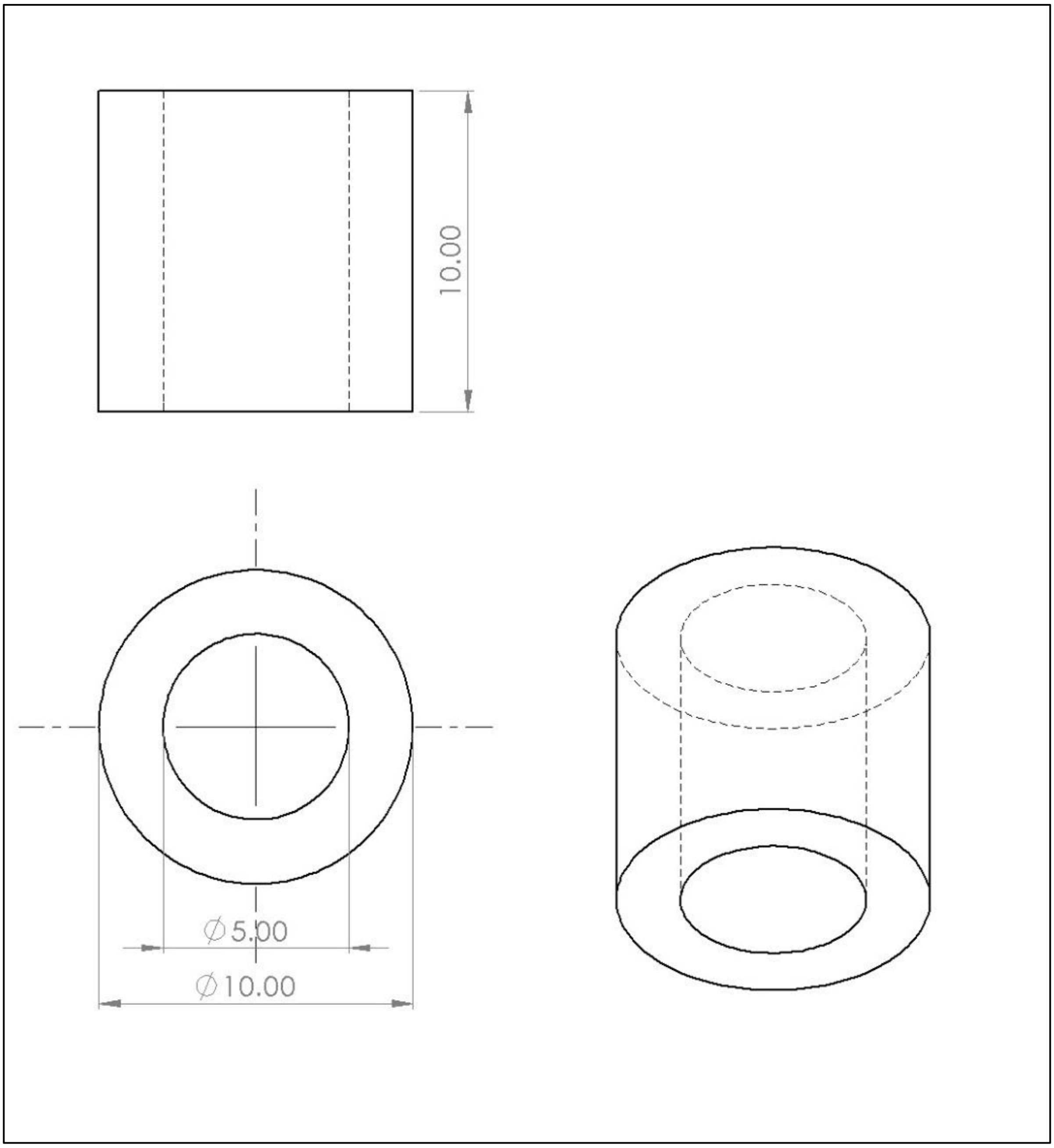

Figure 15: Drawing of the coil core

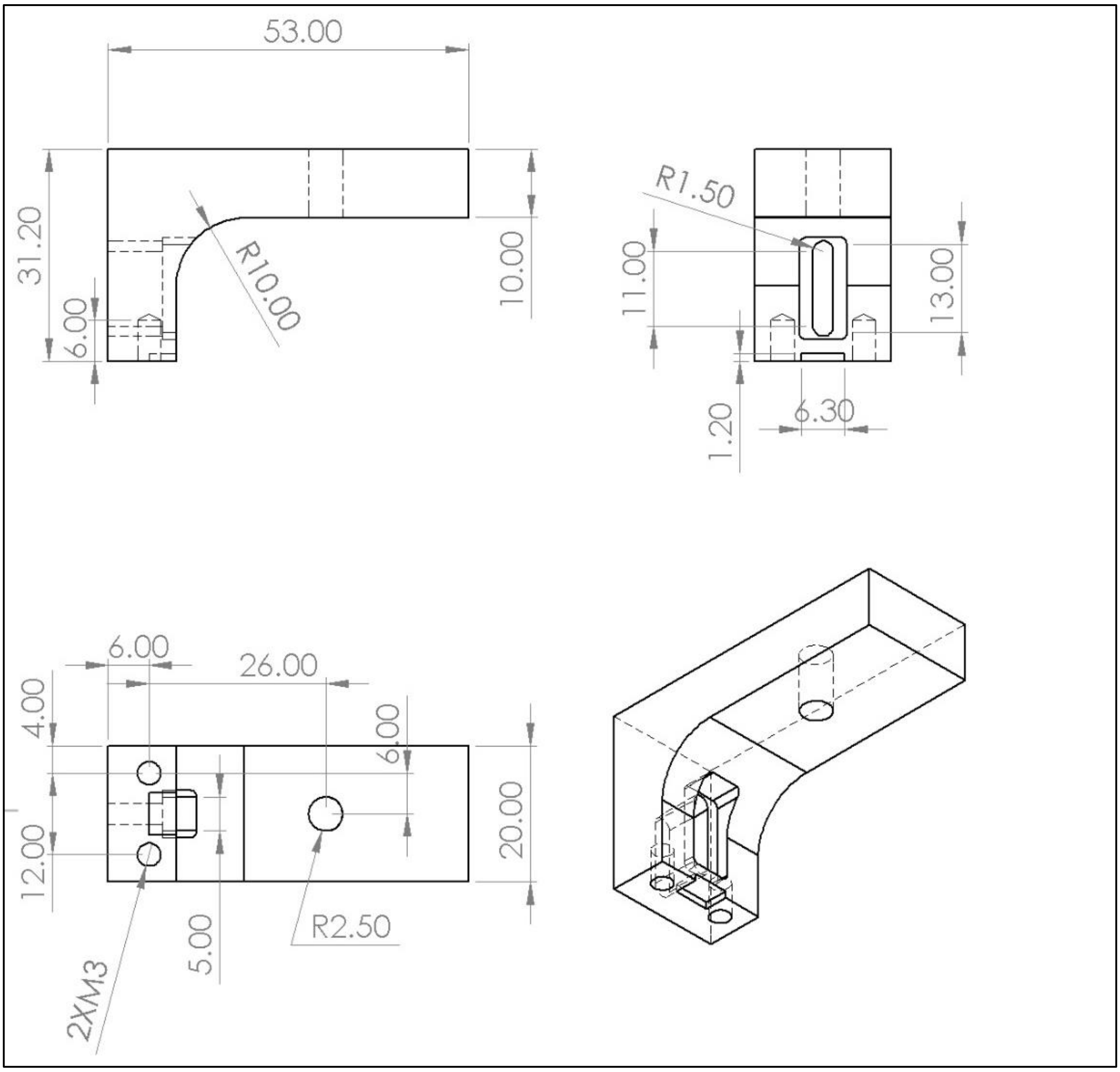

Figure 16: Drawing of the coil holder

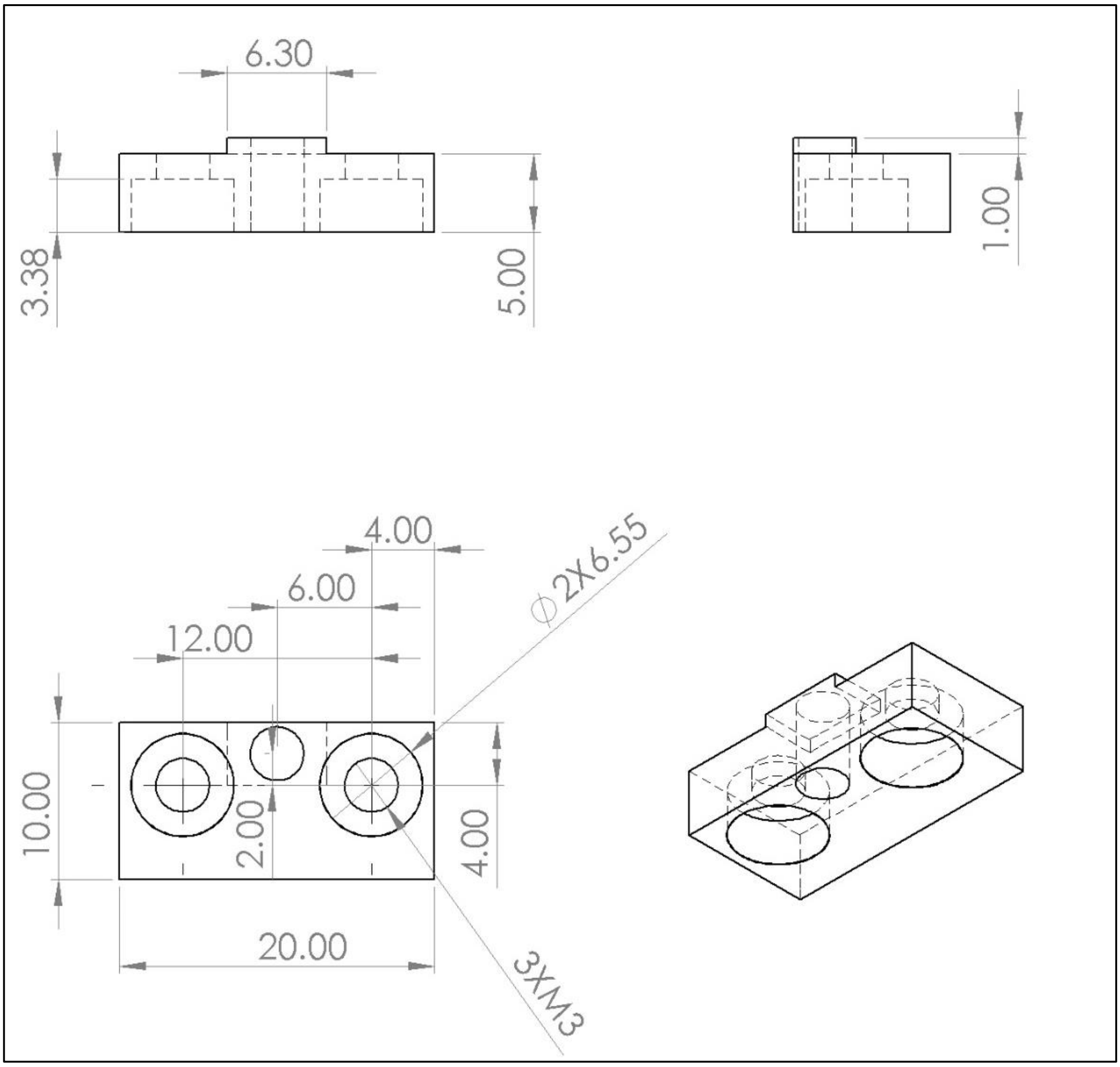

Figure 17: Drawing of the base